



The Society shall not be responsible for statements or opinions advanced in papers or discussion at meetings of the Society or of its Divisions or Sections, or printed in its publications. Discussion is printed only if the paper is published in an ASME Journal. Authorization to photocopy material for internal or personal use under circumstance not falling within the fair use provisions of the Copyright Act is granted by ASME to libraries and other users registered with the Copyright Clearance Center (CCC) Transactional Reporting Service provided that the base fee of \$0.30 per page is paid directly to the CCC, 27 Congress Street, Salem MA 01970. Requests for special permission or bulk reproduction should be addressed to the ASME Technical Publishing Department.

95-GT-339

Copyright © 1995 by ASME

All Rights Reserved

Printed in U.S.A.

ENHANCED MIXING OF 2D LOBED NOZZLES

Liu Huo-Xing and Wu Shou-Sheng
Beijing University of Aeronautics and Astronautics
Department of Jet Propulsion
Beijing, 100083, China

ABSTRACT

The jet axial velocity decay and velocity distributions of two 2D Lobed Nozzles (2DLN), and three baseline nozzles, one circular and two rectangular with different aspect ratios (AR), were measured and compared at low velocity ($M_0 < 0.35$) and ambient temperature conditions. The five nozzles have the same exit area. Test results show:

1) The jet axial velocity decay of the 2DLN may be characterized by three distinct regions; i.e., "potential core region", where the jet axial velocity almost remains constant; "rapid decay region", where streamwise and normal vortices play major roles for enhanced mixing; and, "smooth-down decay region", where the mixing process is dominated by viscous shear layer spreading and small-scale turbulence.

2) The jet potential core length of the two 2DLN tested is only half to one-third that of the baseline rectangular nozzle ($AR=4.37$), and about one-fourth to one-sixth compared with the baseline circular nozzle. The length, in which the jet mixed with surrounding air is nearly uniform, is one to two times that of the 2DLN equivalent exit diameter, and depends on lobe design.

INTRODUCTION

Enhanced mixing between two flows has significance in gas turbine fields; e.g., in the combustion and exhaust systems of gas turbine engines. It can result in jet noise reduction, thrust augmentation, and size reduction. A large amount of research work in this area has been done in the past. It is found that the lobed nozzle (Fig.1) has

very good mixing performance between inner and outer flows. The past research work on the enhanced mixing mechanism of the lobed nozzle showed that:

1. The lobed nozzle has much larger circumference in comparison with conventional nozzles (circular or rectangular nozzle) having same exit area. The longer initial interface between two mixing flows will promote the development of mixing shear layer, and then, enhanced mixing.

2. The convoluted exit shape of the lobed nozzle can induce a large scale streamwise vortex array, which significantly enhances the mixing with less pressure loss.

3. The normal vortex, which belongs in the Kelvin-Helmholtz instable vortex, sheds periodically from the convoluted trailing edge of the lobed nozzle, and also plays an important role in the enhanced mixing process.

The past research work on the application of the lobed nozzle also showed that the lobed nozzle can effectively reduce jet noise and increase engine thrust; and it only needs a mixing distance about 1-2 times the nozzle equivalent exit diameter for nearly uniform mixing.

Tillman et al. (1988) tested and compared the global mixing characteristics, i.e. the temperature, pressure distribution and decay characteristics, of exhaust jets from circular, rectangular, sawtooth and splayed (one type of forced mixer nozzle which also generates large-scale streamwise vortex array downstream of the exit) nozzles at supersonic conditions. Results showed that the large-scale streamwise vortex array also plays a major role in the enhanced mixing process at supersonic conditions. The jet potential core length of the splayed nozzle is only half that of the baseline rectangular nozzle.

This paper will describe and analyse the experimental results on the global mixing characteristics of jets

exhausted from two types of 2DLN and three baseline nozzles (one circular and two rectangular nozzles with different AR) at low velocity and ambient temperature conditions ($t_a = 17-20^\circ\text{C}$).

EXPERIMENTAL ARRANGEMENT

Test rig and measurement

The experimental research was carried out on the low velocity, hot jet test rig in BUAA. The rig system was shown in Fig.2. Its maximum air mass flow rate is 0.9kg/s , with an exhaust gas temperature up to 800°C . However, only cold test was required in the experiment, therefore, the combustor (5) and fuel supply system of the rig was not used.

The main parameters required in the experiment were: mass flow rate of the primary air, air temperature and pressure (especially at the inlet of the test model), and the axial velocity of the exhaust jet. The air mass flow rate was obtained by the flow nozzle (4), in which a thermocouple and a pitot tube were installed to measure the air temperature and pressure for calculating the air density, velocity, and mass flow rate. The axial velocity distribution of the exhaust jet was acquired by a pressure rake horizontally installed on a manual 3D traverse mechanism, which can move the rake along three coordinate axes.

The pressure rake has twelve points transversely, uniformly distributed. By traversing the pressure rake up and down (Z-direction), and along jet axial direction X, the whole pressure field of the exhaust jet can be measured, and then, the axial velocity field of the exhaust jet can be calculated.

Test models

Five nozzle models (Fig.3) were used for the experiment: two 2DLN (2D Opposed Lobed Nozzle, (2DOLN, Fig.3a) and 2D Single-Ramp Lobed Nozzle (2DSRLN, Fig.3b)); and, three baseline nozzles (one Circular Nozzle (CN, Fig.3c) and two Rectangular Nozzles (RN-A, $AR=2.65$, Fig.3d and RN-B, $AR=4.37$, Fig.3e)). The five nozzle models were designed to have same nozzle exit area, (6400 square mm), or same equivalent nozzle exit diameter (90mm), to ensure the experimental results were comparable.

Experimental procedure

In the experiment, a 12-point pressure rake, which was initially horizontally installed at the symmetric axis of

the nozzle exit for the circular and rectangular nozzles and at the half lobe height of the nozzle exit for 2DLN (see Fig.4), was intermittently moved downstream until an axial distance of about 500mm. After each move, a set of data was recorded, and then, the jet axial velocity decay characteristics of tested nozzle was determined.

At three axial locations; i.e, nozzle exit ($x=0$), downstream 90mm ($x=90\text{mm}$) and 140mm ($x=140\text{mm}$), the jet axial velocity distribution of tested nozzle was obtained by traversing the pressure rake vertically. After every 10mm move, a set of data was recorded.

RESULTS AND DISCUSSION

Jet axial velocity decay characteristics

Sforza et al.(1966) and Tillman et al.(1988) have reported the jet decay characteristics of circular and rectangular nozzles. Figure 5 shows the jet axial velocity decay characteristics of circular nozzle obtained by our experiment. Three curves a, b and c shown in Fig.5 represent the decay characteristics at three transverse points, i.e. nozzle center, 15.4mm and 30.8mm off the center, respectively. In Figs.5-11, symbol V is local axial velocity measured, and $V_{x=0}$ is axial velocity measured at nozzle exit. It can be seen from Fig.5 that the farther the measured point is off center, the shorter the potential core length is, and the steeper the velocity decay slope in decay region is. Maximum potential core length (at axis) is about 300mm.

The jet axial velocity decay characteristics of two rectangular baseline nozzles obtained by our experiment are given in Figs.6 and 7. It can be seen from the figures that the maximum potential core lengths (at axis) of the two rectangular nozzles are about 180mm (RN-A) and 150mm (RN-B), respectively. This indicates that nozzles with larger AR have shorter potential core length; and, maximum potential core length of RN-A and RN-B are only 0.6 and 0.5 times that of circular nozzle. This trend is in agreement with the data of Sforza and Stasi (1979) and Tillman et al.(1988), which show approximately a factor of two difference between the potential core length of rectangular nozzle ($AR=3.7$) and circular nozzle ($AR=1.0$).

Another feature, which is obviously different from the circular nozzle, of the jet axial velocity decay characteristics of rectangular nozzles is that there are critical axial distances existing for the all nine measured transverse points of two rectangular nozzles. The jet axial velocity is nearly constant before the critical distance and

after that, the jet axial velocity decay and decay rate increase with the measured point transversely farther off the center. Comparing Fig.6 with Fig.7, it is found that the effect of the measured point transversely off the center on the critical distance is less with the increase of AR. For example, the critical distances of five measured points for the RN-B of AR=4.37 are near the same, but for the RN-A of AR=2.65, the critical distance is shorter with the measured point transversely farther off the center.

The jet axial velocity decay characteristics of two experimental 2DLN are shown in Figs.8 and 9. They are different from that of baseline circular and rectangular nozzles, and can clearly be divided into three distinct regions.

1. Potential region (where the jet axial velocity is constant). The length of this region is very short in comparison with the baseline circular and rectangular nozzles tested. It is only about 50mm for 2DOLN and 70mm for 2DSRLN. This means that potential core length of 2DLN tested is only about 1/4-1/6 that of circular nozzle, and about 1/2-1/3 that of the rectangular nozzle with AR around 4.0. This region is seen as the formation region of a streamwise vortex .

2. Rapid decay region (where jet axial velocity rapidly decays with the increase of axial distance X). Forty percent (40%) axial velocity decay only needs a distance of 70mm for 2DOLN, and 45% axial velocity decay needs a distance of 130mm for 2DSRLN in this region (see Figs.8 and 9). Obviously, the rapid decay of jet axial velocity is owing to the effects of streamwise and normal vortices mentioned by McCormick and Bennett (1993). Therefore, this region can be seen as enhanced mixing region by vorticity. Comparing Fig.8 with Fig.9, one can also see that the decay rate of jet axial velocity of 2DOLN is higher than that of 2DSRLN at this region. This indicates that the effectiveness of enhanced mixing of 2DOLN is better than that of 2DSRLN.

3. Smooth-down decay region (where the jet axial velocity smoothly decays). This indicates that the effects of the streamwise and normal vortices, induced by the lobes, disappears and the decay of jet axial velocity at this region is caused by conventional shearing layer spreading and small-scale turbulence.

The above concept of the three distinct regions for the jet exhausted from lobed nozzles conforms and complements each other, from different viewpoint, with the concept of the three regions (or stages) put forward by Werle et al. (1987) and Eckerle et al.(1990), for vortex development downstream of lobes.

The division of above three characteristic regions of the

2DLN jet should also be applicable to an axisymmetric lobed nozzle (not tested) due to both having the same mechanism of enhanced mixing.

In addition, it can also be seen from Figs.8 and 9 that the jet axial velocity decay characteristics of measured points b and c, which correspond to the two middle lobes of 2DLN, are nearly the same; and, the decay characteristics of measured points a and d, which correspond to the two side lobes of 2DLN, are nearly the same as well. However, there are certain differences between the a,b, and c,d curves, especially in the smooth-down decay region, where the decay slopes of a and d curves are higher than that of b and c curves. The side wall and the effect of thick boundary layers on these walls on the subsequent development of properties of the jet down stream could be the reason. At the potential core region, the four decay curves (a, b, c and d) of two 2DLN also appear to have another feature, a measurable axial velocity increase, which especially clear for curves a and d corresponding to the two side lobes.

Figure 10 puts the jet axial characteristics of the five test nozzles together, and more clearly shows the features and differences of them.

Jet axial velocity distribution at different cross-sections

The jet axial velocity distributions of the circular, and rectangular (RN-A) nozzles, tested at three cross-sections, are shown in Figs.11 and 12 respectively. It can be seen from the figures that the area of high velocity potential core contracts with the increase of axial distance X.

Figures 13 and 14 are the jet axial velocity distributions of 2DOLN and 2DSRLN at three cross-sections, respectively. The axial velocity distributions of two 2DLN at nozzle exit ($x=0$) are basically determined by the exit shape of lobes. High velocity potential core areas are near the centers of the four lobes and in the gap between lobe and ramp. However, the jet axial velocity distributions of the two 2DLN at $x=140$ mm are rather uniform. High velocity areas appeared at $x=0$ have basically disappeared at $x=140$ mm, and only small trace spots can be found in the figures. The high velocity trace spots of 2DOLN jet are smaller and lower than that of 2DSRLN jet. This also indicates that the enhanced mixing of 2DOLN is stronger than that of 2DSRLN. Contrasting with the jet axial velocity decay characteristics of the two 2DLN mentioned above, the 2DOLN jet at $x=140$ mm has entered smooth-down decay region, but the 2DSRLN jet is still in rapid decay region.

It can be anticipated that the mixing uniformity of the 2DOLN at $x=140\text{mm}$ should be reached by 2DSRLN jet around $x=200\text{mm}$.

Comparing the jet axial velocity distribution of 2DOLN with that of 2DSRLN at $x=90\text{mm}$, it can also be seen that the mixing uniformity of the 2DOLN jet is better than that of 2DSRLN jet as well. The jet axial velocity distribution of 2DSRLN at $x=90\text{mm}$ is almost similar to that at $x=0$, and only the velocity contour has a little extension along lobe height. Although the jet axial velocity distribution of the 2DOLN at $x=90\text{mm}$ still shows the effect of lobe shape, it has had obvious changes in comparison with that at $x=0$. This also can be explained by comparison Fig.9 with Fig.10. The jet axial velocity decay characteristics of 2DOLN at $x=90\text{mm}$ has entered rapid decay region, but that of 2DSRLN at $x=90\text{mm}$ is still in potential core region where the enhanced mixing effect of vorticity is not yet effective.

Figure 15 shows the axial velocity distribution along transverse coordinate Y with different axial distance X at the half height of 2DSRLN lobes. It displays, from another aspect, the feature of the 2DLN jet axial velocity field. There are four velocity peaks existence corresponding to the four lobe axis locations at $x=100\text{mm}$. Velocity profile at $x=200\text{mm}$ has a saddle-type, i.e. lower velocity in the center and two smaller velocity peaks at both side corresponding to the inner interface of two side lobes. The velocity profile at $x=300\text{mm}$ is almost uniform.

CONCLUSION

The following two conclusions can be obtained from the experiment:

1. The jet axial velocity decay of lobed nozzles can be characterized by three distinct regions; i.e., "potential core region", where the jet axial velocity almost keeps constant; "rapid decay region", where streamwise and normal vortices play major roles for enhanced mixing; and, "smooth-down decay region", where the mixing process is dominated by viscous shear layer spreading and small-scale turbulence.

2. The jet potential core length of the two 2DLN tested is only half to one-third related to the baseline rectangular nozzles ($AR=4.37$), and about one-fourth to one-sixth compared with the baseline circular nozzle. The length, in which jet mixed with surrounding air is nearly uniform, is one to two times of 2DLN equivalent exit diameter, and depends on lobe design.

REFERENCE

- Eckerle, W.A., Sheibani, H. and Awad, J., "Experimental Measurement of the Vortex Development Downstream of a Lobed Forced Mixer", ASME 90-GT-27.
- McCormick and John C. Bennett, Jr. (1993), "Vortical and Turbulent Structure of a Lobed Mixer Free-Shear Layer", AIAA-93-0219.
- Sforza, P.M., Steiger, M.H., and Trentacoste, N. (1966), "Studies on Three-Dimensional Viscous Jets", AIAA Journal, Vol.4, pp.800-806.
- Sforza, P.M., and Stasi, W. (1979), "Heated Three-Dimensional Turbulent Jets", Journal of Heat Transfer, Vol.101, pp.353-358.
- Tillman, T.G., Patrick, W.P. and Paterson, R.W. (1988), "Enhanced Mixing of Supersonic Jets", AIAA-88-3002.
- Werle, M.J., Parterson, R.W. and Presz, Jr. W.M., "Flow Structure in a Periodic Axial Vortex Array", AIAA-87-0610.

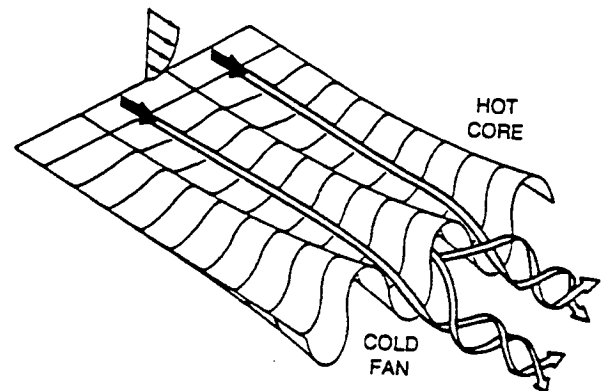


Fig.1 Enhanced mixing scheme of lobed nozzles

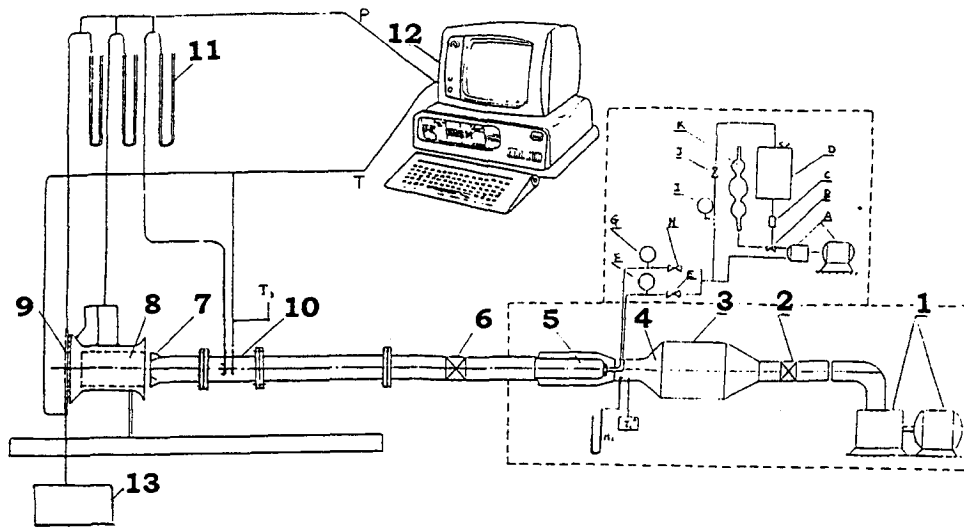


Fig.2 Schematic test rig system

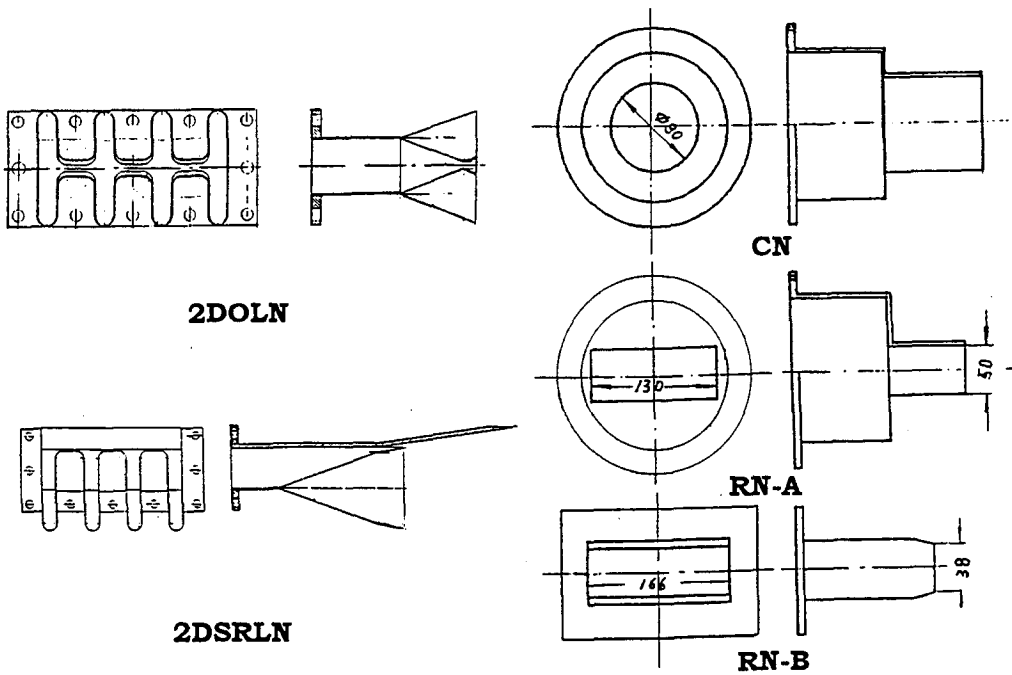


Fig.3 Test models

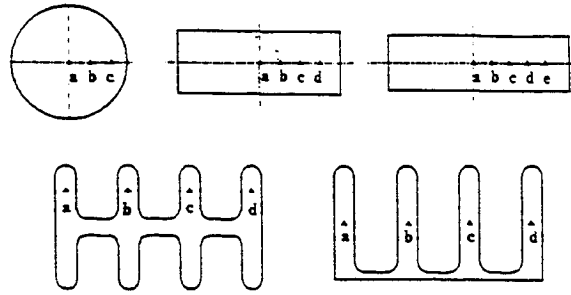


Fig.4 Measured locations of five nozzles

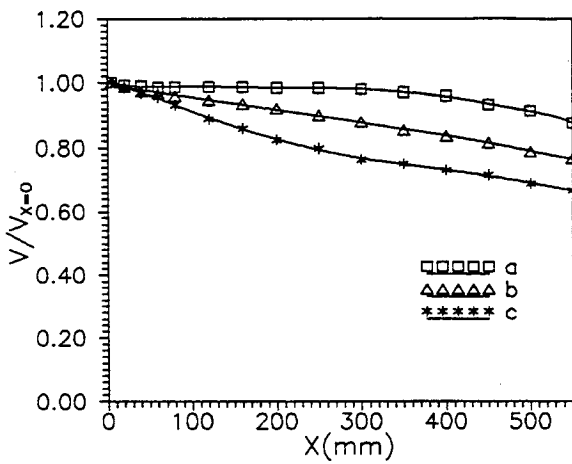


Fig.5 Jet axial velocity decay characteristics of CN

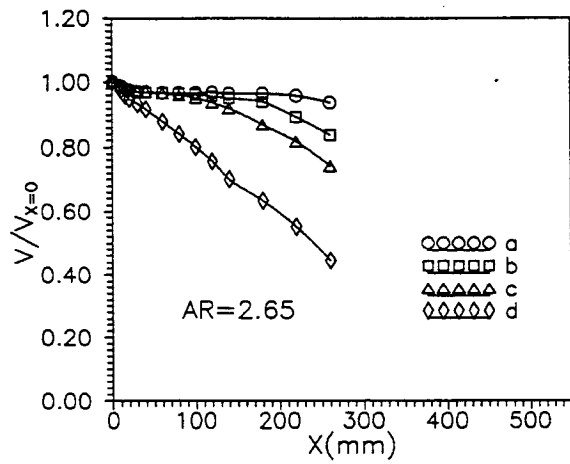


Fig.6 Jet axial velocity decay characteristics of RN-A

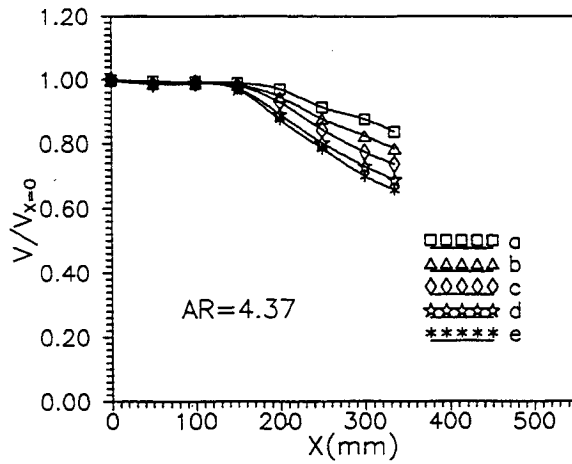


Fig.7 Jet axial velocity decay characteristics of RN-B

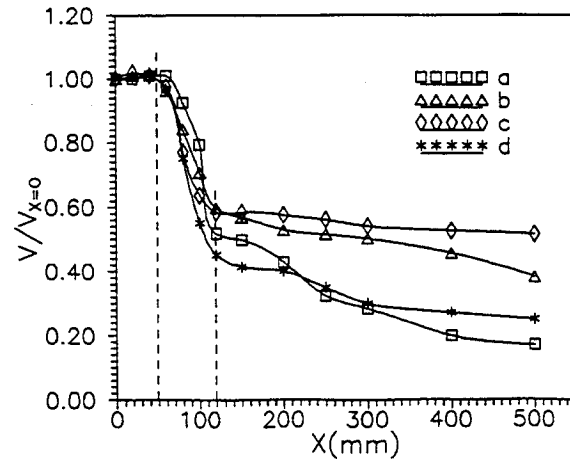


Fig.8 Jet axial velocity decay characteristics of 2DOLN

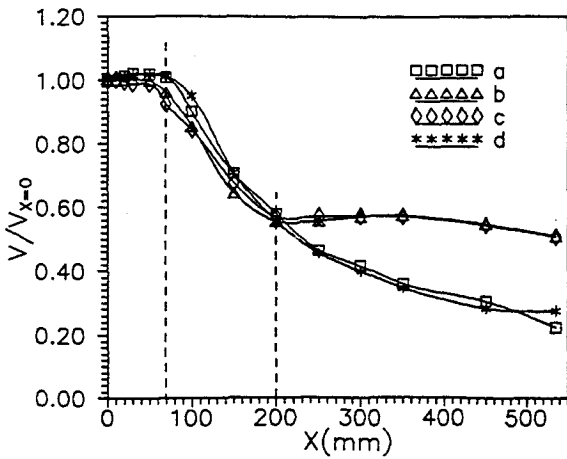


Fig.9 Jet axial velocity decay characteristics of 2DSRLN

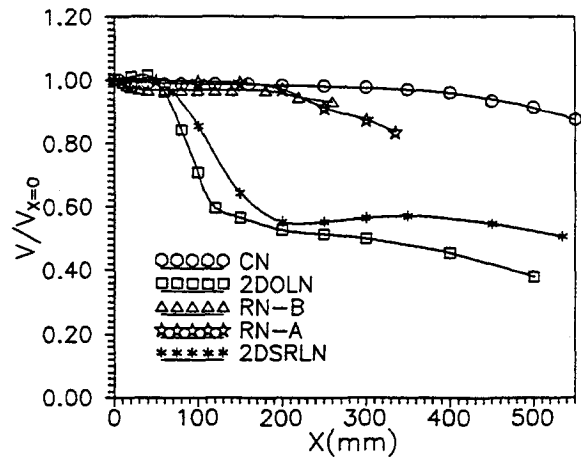


Fig.10 Jet axial velocity decay characteristics of five nozzles

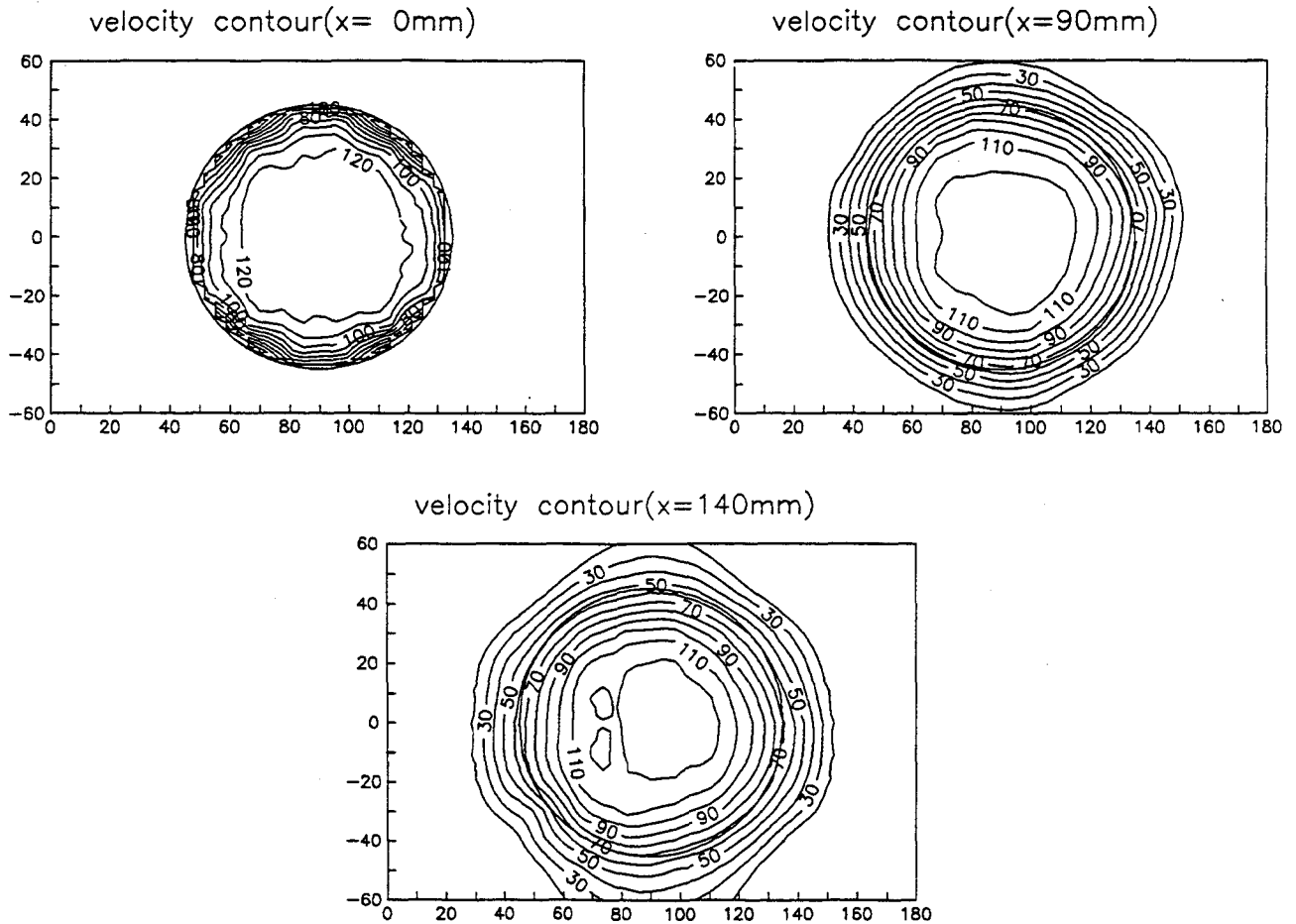


Fig.11 Jet axial velocity distributions of CN

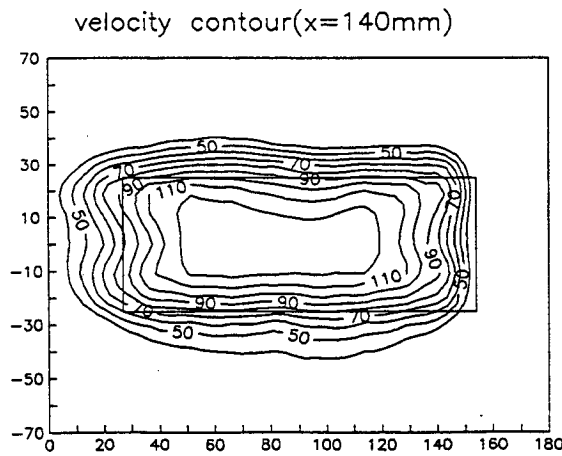
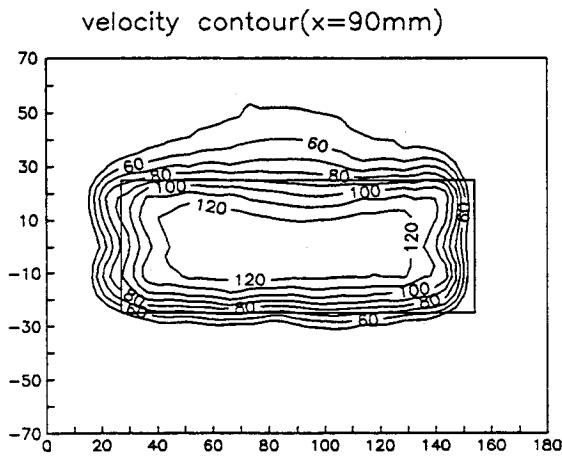
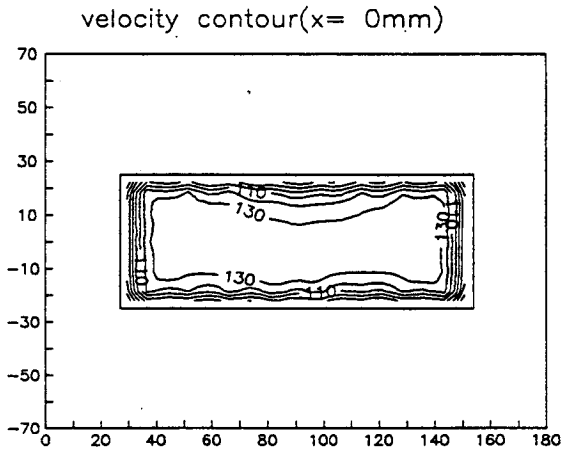


Fig.12 Jet axial velocity distributions of RN-A

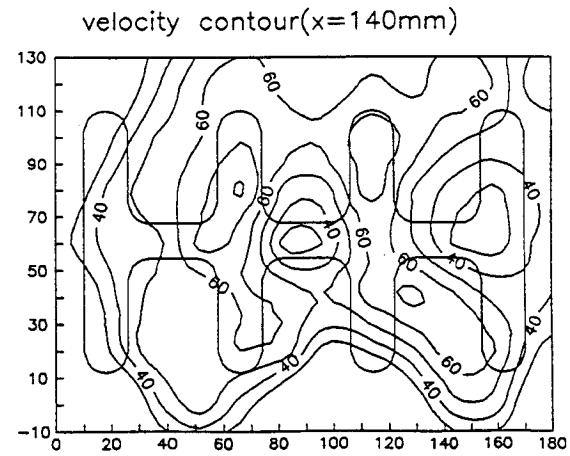
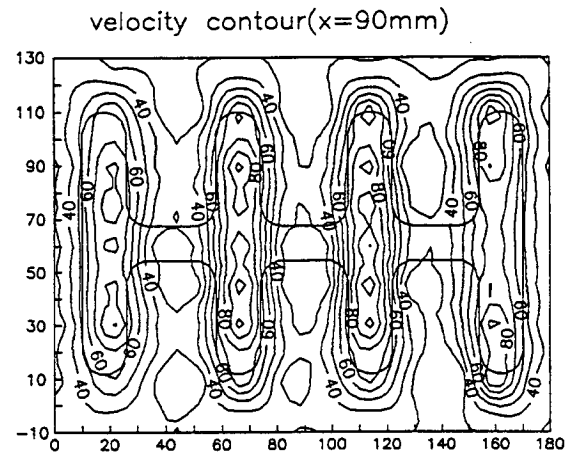
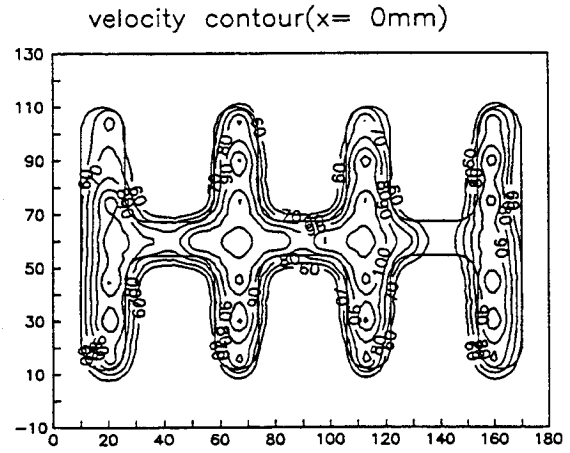


Fig.13 Jet axial velocity distributions of 2DOLN

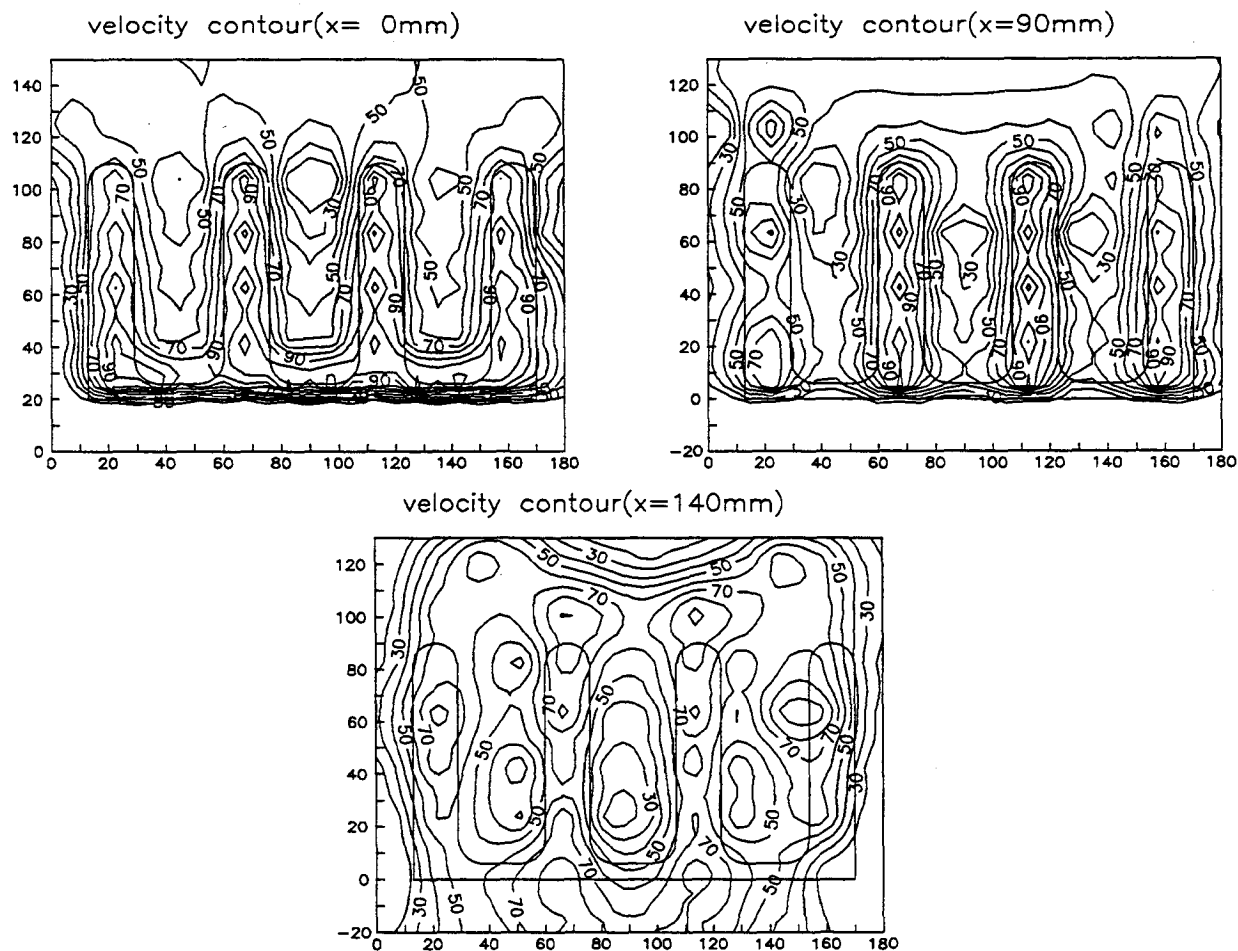


Fig.14 Jet axial velocity distributions of 2DSRLN

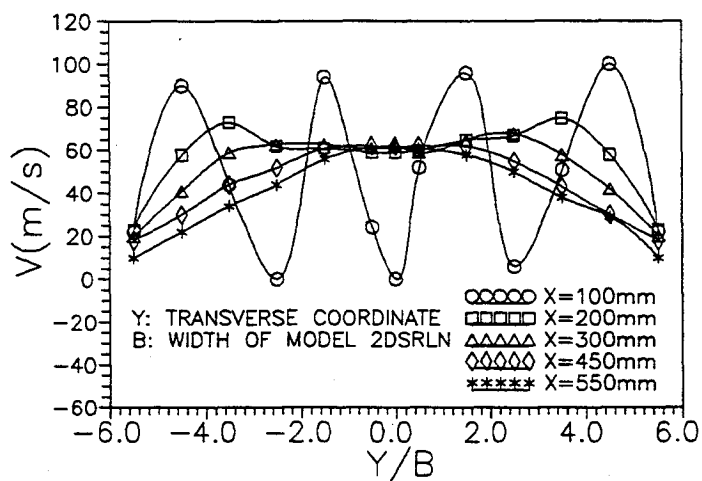


Fig.15 Jet axial velocity distributions of X-Y plane of 2DSRLN